Virology 385 (2009) 143–154

Contents lists available at ScienceDirect

Virology

journal homepage: www.elsevier.com/locate/yviro

Betanodavirus non-structural protein B2: A novel necrotic death factor that induces mitochondria-mediated cell death in fish cells

Yu-Chin Su [a], Jen-Leih Wu [b], Jiann-Ruey Hong [a,*]

[a] Laboratory of Molecular Virology and Biotechnology, Institute of Biotechnology, National Cheng Kung University, Tainan 701, Taiwan, ROC
[b] Laboratory of Marine Molecular Biology and Biotechnology, Institute of Cellular and Organismic Biology, Academia Sinica, Nankang, Taipei 115, Taiwan, ROC

ARTICLE INFO

Article history:
Received 14 August 2008
Returned to author for revision
17 September 2008
Accepted 13 November 2008
Available online 29 December 2008

Keywords:
Nervous necrosis virus
siRNA silencing suppressor B2
Mitochondrial membrane potential
Bax
siRNA

ABSTRACT

The Betanodavirus non-structural protein B2 plays a role in silencing RNA interference (RNAi), which mediated regulation of animal and plant innate immune responses, but little is known regarding the role of B2 in cell death. The present study examined the effects of B2 on mitochondria-mediated necrotic cell death in grouper liver (GL-av) cells. *B2* was expressed at 12 h post-infection (pi), with increased expression between 24 and 72 h pi by Western blot. B2 was transiently expressed to investigate possible novel protein functions. Transient expression of B2 in GL-av cells resulted in apoptotic cell features and positive TUNEL assays (28%) at 24 h post-transfection (pt). During mechanistic studies of cell death, B2 upregulated expression of the proapoptotic gene *Bax* (2.8 fold at 48 h pt) and induced loss of mitochondria membrane potential (MMP) but not mitochondrial cytochrome *c* release. Furthermore, over expression of Bcl-2 family member *zfBcl-xL* effectively prevented B2-induced, mitochondria-mediated necrotic cell death. Finally, using RNA interference to reduce B2 expression, both *B2* and *Bax* expression were downregulated and RGNNV-infected cells were rescued from secondary necrosis. Taken together, our results suggest that B2 upregulates *Bax* and triggers mitochondria-mediated necrotic cell death independent of cytochrome *c* release.

Introduction

The Nodaviridae family of viruses contains two genera: betanodaviruses, which predominantly infect fish, and alphanodaviruses, which mostly infect insects (Ball and Johnson, 1999; Schneemann et al., 1998). Betanodaviruses are the causative agents for viral nervous necrosis (VNN), an infectious neuropathological condition characterized by necrosis of the central nervous system, including the brain and retina, which presents with clinical signs including abnormal swimming behavior and darkening of the fish (Bovo et al., 1999). This disease is capable of causing massive mortality in the larvae and juvenile populations of several marine teleost species worldwide (Munday et al., 2002). Disease manifestation may correlate with innate or acquired immunity (Lu et al., 2008; Poisa-Beios et al., 2008).

The nodavirus genome is bipartite, comprised of two molecules of SINGLE stranded, positive polarity RNA (RNA1 and RNA2) approximately 3.1 and 1.4 kb, respectively, in length, and lacking a 3′ poly (A) extension (Mori et al., 1992). RNA1 encodes an approximately 100 kDa non-structural protein that has been designated RNA-dependent RNA polymerase (RdRp) or protein A. This protein is vital for replication of the viral genome. RNA2 encodes a 42 kDa capsid protein (Mori et al., 1992; Delssert et al., 1997).

Alpha nodavirus synthesize a sub-genomic RNA3 from the 3′ terminus of RNA1 during RNA replication which encodes two small proteins, B1 and B2 (Ball and Johnson, 1999; Schneemann et al., 1998; Johnson et al., 2000), but up to now, in beta nodaviruses just encode a B2 protein only (Iwamoto et al., 2005). B2 can function as a host siRNA silencing suppressor in alphanodaviruses, including the nodaviruses flock house virus (FHV) and Nodamura virus (NoV); striped jack nervous necrosis virus (SJNNV) also inhibits silencing of viral RNAs in insect, mammalian, and plant cells (Iwamoto et al., 2005; Li et al., 2002; Lu et al., 2005; Wang et al., 2006). However, the underlying mechanism of B2 as a siRNA silencing suppressor blocking the host innate immune defense system is unclear, as are any other putative functions of this protein.

Apoptosis is controlled at the mitochondrial level by the sequestration of a series of apoptogenic proteins, including cytochrome c, Smac/DIABLO, apoptosis inducing factor (AIF), and endonuclease G in the mitochondrial intermembrane space, which allows the cytosolic release of these factors upon exposure to proapoptotic signals (Wang, 2001; Ferri and Kroemer, 2001). The Bcl-2 family of proteins consists of both anti- and pro-apoptotic molecules. These proteins form a critical intracellular decision point regulating responses to common cell death pathways (Farrow and Brown, 1996). The ratio of antagonist (Bcl-2, Bcl-xL, Mcl-1, and A1) to agonist (Bax, Bak, Bcl-x_s and Bad) molecules dictates whether a cell responds to a proximal apoptotic stimulus (Farrow and Brown, 1996; Oltvai et al., 1993). These proteins also interact with mitochondria to

* Corresponding author. Fax: +886 6 2766505.
E-mail address: jrhong@mail.ncku.edu.tw (J.-R. Hong).

0042-6822/$ – see front matter © 2008 Elsevier Inc. All rights reserved.
doi:10.1016/j.virol.2008.11.036

control the balance of mitochondrial membrane potential (MMP) (Zamzami and Kroemer, 2001). Bax and Bak can function redundantly in the release cytochrome c from mitochondria in response to various inducers of apoptosis (Wei et al., 2001; Keep et al., 2007).

The red-spotted grouper nervous necrosis virus (RGNNV) TN1 strain induces host apoptosis which precedes the onset of necrosis in a grouper liver cell line (GL-av) (Chen et al., 2006a). This process can activate the mitochondrial permeability transition pore, but can be blocked by the adenine nucleotide translocase (ANT) inhibitor BKA (Chen et al., 2006a) and by the mitochondria membrane stabilizer zfBcl-xL, a member of the Bcl-2 protein family (Chen et al., 2006b, 2007). Although Protein α can trigger cell death (Guo et al., 2003), zfBcl-xL overexpression can rescue Protein α-induced MMP loss in fish cells (Wu et al., 2008).

Interestingly, this process of necrosis during RGNNV infection, which can mediate loss of mitochondria, can be blocked by the protein synthesis inhibitor cycloheximide (CHX) in a manner that is strongly correlated with RGNNV B2 protein expression (Chen et al., 2007). Aside from B2's recognized role as a suppressor of siRNA silencing, the protein's role in the regulation of the necrotic death in GL-av cells infected by RGNNV is unclear (Chen et al., 2007). In the present study, we demonstrate a new function for B2. B2 upregulates the expression of the pro-apoptotic Bax and induces the loss of MMP, which may trigger mitochondria-mediated necrotic cell death at the mid-to-late stages of viral replication. These findings may provide new insight into betanodavirus-induced pathogenesis.

Results

Cloning of RGNNV B2

Cloning of the genetic region including *B2* yielded a 228 nt region encoding a 75 amino acid protein with an approximate molecular weight of 8.5 kDa and a theoretical pI value of 5.20. When the amino acid identity of B2 from the RGNNV TN1 strain (A; AAX77498.1) was compared with other species, a 98% match was found for RGNNV (B; AAK21878.1), a 98% match for the SGNNV (C; AAQ90062.1), a 90% match for AHNNV (D; CAD66426.1), and a 80% match for SJNNV (E; BAB64330.1). Possible protein modification sites in the B2 protein included a N-myristoylation site (30–35 aa, GGVTAI; Box A), a protein kinase C phosphorylation site (58–60 aa, SRR; Box B), casein kinase II phosphorylation sites (66–69 aa, TVIE; Box C), and a mitochondrial specific sequence (42–52 aa, TFVISHAAA; E Box) (Fig. 1B) (Falquet et al., 2002).

RGNNV B2 upregulates Bax expression and induces loss of MMP in necrotic fish cells

B2 was fused with EYFP and the resulting fusion gene was utilized to directly monitor B2-induced cell morphological changes. Expression of the approximately 40.4 kDa EYFP-B2 fusion protein was detected 24 h post transfection (pt) by Western blot (Fig. 2A, lane 3). Expression of EYFP-B2 in grouper fish liver (GL-av) cells caused apoptotic cell death at 24 h pt (Fig. 2B:f; arrows) which did not occur in cells transfected with EGFP (Fig. 2B:e). EYFP-B2-mediated induction of apoptotic cell death was further confirmed using the TUNEL assay (Fig. 2B). TUNEL-positive cells (indicated by arrows) showed EYFP-B2 expression and only rarely EYFP expression (Fig. 2B:a and c) that corresponded to the percentages of TUNEL-positive cells at 0, 24, 48, and 72 h pt (Fig. 2C). In the EYFP-B2 transfection groups, TUNEL-positive cells gradually increased with increased time pt (1% at 0 h, 28% at 24 h, 35% at 48 h, and 44% at 72 h) as compared with the EGFP control (Fig. 2C:a; 1% at 0 h, 2.5% at 24 h, 2% at 48 h, and 2% at 72 h pt). In NIH3T3 cells, B2 expression also caused apoptotic cell death (data not shown).

During this screening, we found that B2 expression dramatically upregulated (up to 3-fold) the proapoptotic Bax at 48 h pt (Fig. 3, lane 7) as compared to negative control cells transfected with the vector only (Fig. 3, lanes 2–4, at 0 h, 24 h, and 48 h, respectively). MCF-7 cells were used as a positive control and are presented in Fig. 3, lane 1. Bcl-2 expression was evaluated as a negative control for protein expression. There were minus increased 5% (24 h p.i.; Fig. 3, lane 6) and 10% (48 h p.i.; Fig. 3, lane 7), respectively, in Bcl-2 expression between the vector control group (Fig. 3, lanes 2–4) and the B2 expression group (0 h; Fig. 3, lane 5). Actin expression was used as an internal control (Fig. 3, lanes 2–7). The protein expression amounts were quantified by Personal Densitometer (Molecular Dynamic) from Fig. 3.

B2 protein induced loss of MMP independent of cytochrome c release in fish cells

In order to determine whether B2 expression could induce the loss of MMP in fish cells, mitochondrial function was evaluated between 0 h and 48 h pt. As expected, the MitoCapture dye aggregated and showed red fluorescence in the healthy mitochondria of normal control cells (Fig. 4A:c) and cells transfected with vector only (Fig. 4A:f). However, mitochondrial fluorescence was not evident in apoptotic cells, where the dye remained monomeric in the cytoplasm and showed strong green fluorescence (Fig. 4A:h; open circles). Loss of red fluorescence (Fig. 4A:i; open circles) and enhanced green fluorescence (Fig. 4A:h; open circles) occurred in cells undergoing morphological changes (Fig. 4A:g; open circles) such as gradual loss of flattening (open circles), in contrast to the normal control cells (Fig. 4A:a) and vector control cells (Fig. 4A:d). Loss of MMP cell number were greater in RGNNV B2-transfected cells (1% at 0 h, 28% at 24 h, and 32% at 48 h) than in either the negative control (1% at 0, 24, and 48 h) or the vector control (1% at 0 h, 1.5% at 24 h, and 2% at 48 h) cells (Fig. 4B). In addition, after 48 h of transient expression, the localization of EYFP-B2 and EYFP was identical, which both proteins localized to cytosol (Fig. 4C:a, lane

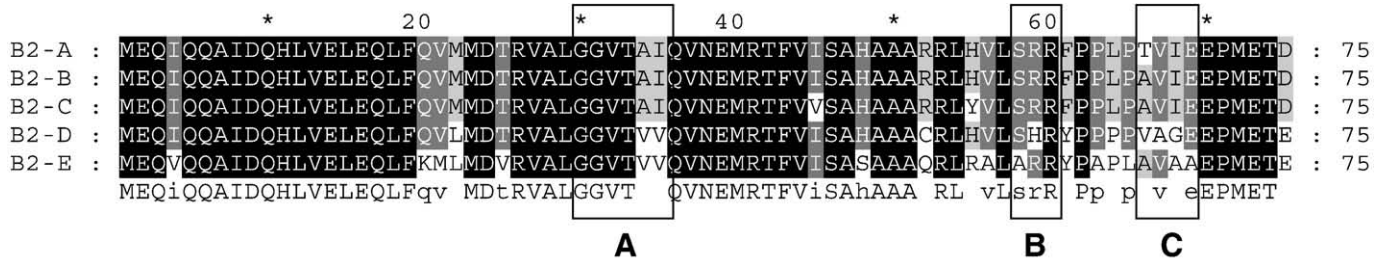

Fig. 1. Cloning and identification of RGNNV B2 as an early expression gene in fish liver cells. Alignment of the deduced amino acid sequence of RGNNV TN1 B2 aligned with the corresponding sequences of other betanodavirus proteins. When we compared the amino acid identity of RGNNV TN1 strain (B2-A) with other species, the match was 98% for RGNNV (B2-B), 98% for SGNNV (B2-C), 90% for AHNNV (B2-D), and 80% for SJNNV (B2-E). The conserved amino acids for residues common to at least five betanodavirus proteins are shown in black blocks and the predicted modification sites A (aa 30–35, myristoylation site), B (aa 58–60, protein kinase C phosphorylation site), C (aa 66–69, casein kinase II phosphorylation site) are underlined.

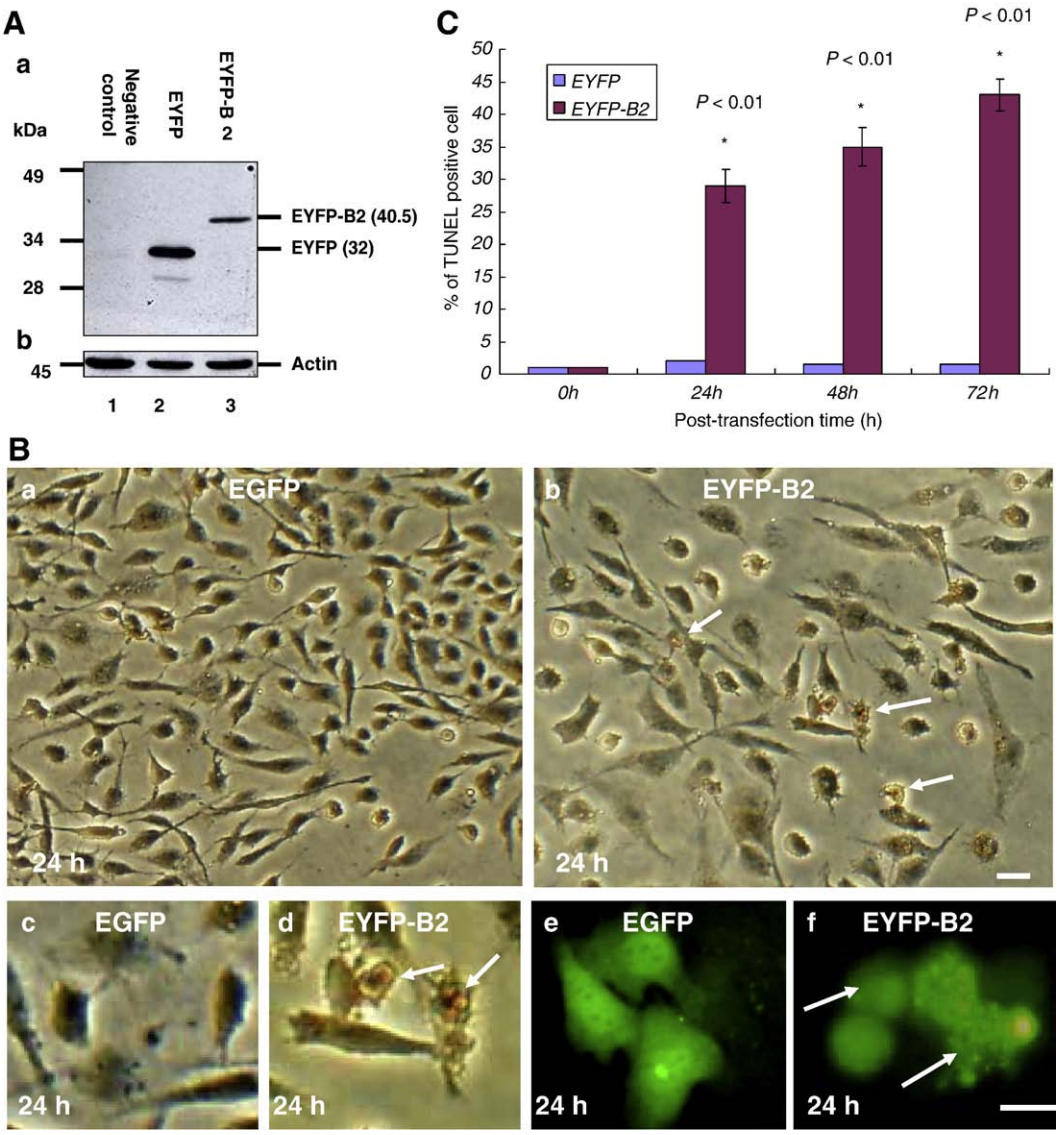

Fig. 2. The B2 protein induces the apoptotic cell death in fish cells. (A) Western blot analysis of EYFP and EYFP-B2 expression in GL-av cells at 24 h pt. (A:a) Lane 1 shows the negative control (no expression), lane 2 shows EYFP, and lane 3 shows EYFP. Actin (the internal control) is shown in A:b. (B) RGNNV B2-induced GL-av cell death as shown by TUNEL-positive brown nuclei (b, d; arrows) at 24 h pi. The normal control is shown in B:a (at 0 h) and 2B:c (at 24 h). (2B:f) The EYFP-B2 fusion gene induced cell death as monitored by green fluorescent protein at 24 h pt. The internal control (EGFP) is shown in B:e. Bar = 10 μm. (C) The number of TUNEL positive nuclei at 0, 24, 48, and 72 h pt, respectively. Data were analyzed using either paired or unpaired Student *t*-tests as appropriate. *p* all >0.01 represented statistically significant differences between mean values of groups.

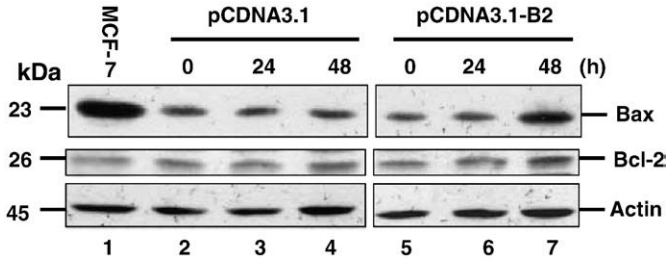

Fig. 3. B2 upregulates the pro-apoptotic gene *Bax* in fish cells. Transfection of RGNNV B2 upregulated *Bax* expression in GL-av cells by Western blot. Lane 1 contained the control MCF-7 cell lysate; lanes 2–4 display transfected pCDNA3.1 plasmid and incubation for 0, 24, and 48 h pi, respectively; lanes 5–7 display transfected pCDNA3.1-B2 plasmid and incubation for 0, 24, and 48 h pi, respectively. Blots were probed with an anti-mouse Bax monoclonal antibody, anti-human Bcl-2 monoclonal antibody, and anti-mouse actin monoclonal antibody.

3: EYFP-B2; lane 2: EYFP) and mitochondria (Fig. 4C:a, lane 6: EYFP-B2; lane 5: EYFP). Negative control cells without EGFP or EYFP-B2 transfection are presented in Fig. 4C:a (lanes 1 and 4, respectively). B2 expression could induce MMP loss but was not required for cytochrome c release (Fig. 4C:b, lane 3 (cytosolic form); lane 6 (mitochondrial form)) as compared with the negative control EGFP-expression group (Fig. 4C:b, lane 2 (cytosolic form); lane 5 (mitochondrial form)) and the non-transfected cells (Fig. 4C:b, lane 1 (cytosolic form); lane 4 (mitochondrial form)) at 48 h pt. Actin (Fig. 4C:c, lanes 1–3) was an internal control for the cytosolic form and cytochrome c oxidase I (Fig. 4C:c, lanes 4–6) for the mitochondrial form.

zfBcl-xL blocked B2-induced MMP loss and cell death

Since Bcl-2 proteins are anti-apoptotic (Newton and Strasser, 1998; Hong et al., 2002), GL-av cells were co-transfected with EGFP-Bcl-xL and EYFP-B2 to test whether Bcl-xL could block B2-induced MMP. The molecular weight of the EYFP-NNV B2 fusion protein was

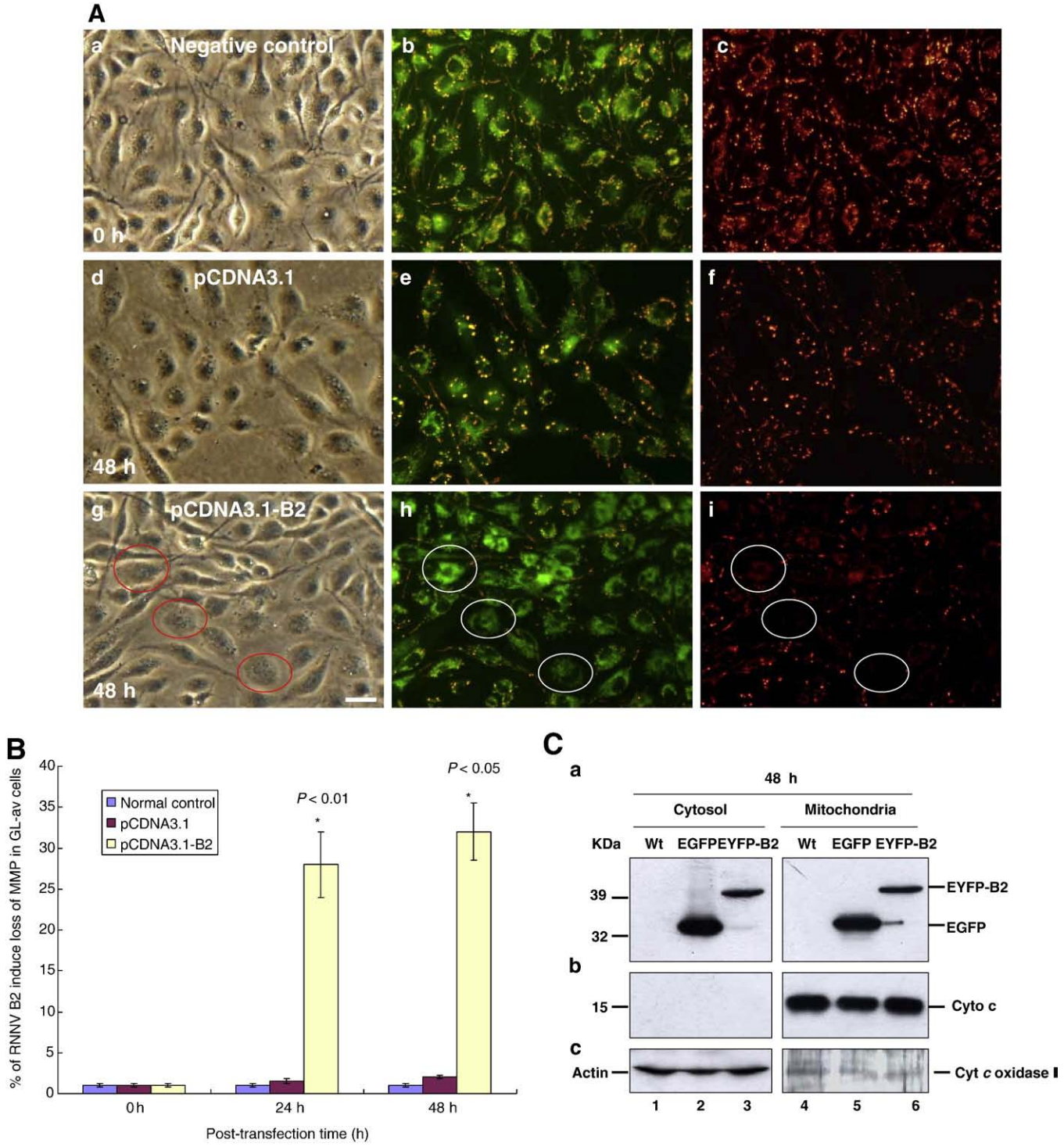

Fig. 4. B2 protein induces loss of MMP in GL-av cells independent of cytochrome *c* release. (A) Identification of B2 protein targeting to mitochondria in GL-av cells, causing loss of MMP at 48 h pt. Negative control cells (A:a–c), pCDNA3.1 vector cells (A: d–f), and RGNNV B2-transfected cells (A: g–i; loss of MMP cells indicated by open cycles). Scale bar = 10 μm. (B) B2 induces loss of MMP in GL-av cells at 0, 24, and 48 h pt. Data were analyzed using either paired or unpaired Student *t*-tests as appropriate. p all <0.05 represented a statistically significant difference between mean values of groups. (C) Western blot analysis of RGNNV B2 induction of the loss of MMP in GL-av cells independent of cytochrome c release. (C:a) Wild type normal control cells (lanes 1, cytosolic form; lane 4, mitochondrial form); EGFP-transfected cells (lane 2, cytosolic form; lane 5, mitochondrial form); and (C:b) RGNNV EYFP-B2-transfected GL-av cells (lane 3, cytosolic form; 6, mitochondrial form). Actin and cytochrome *c* oxidase I internal controls are shown in C (cytosolic form, lanes 1–3; mitochondrial form, lanes 4–6).

approximately 40.4 kDa (Fig. 5A, lanes 2 and 3) and that of the EGFP-Bcl-xL fusion protein was approximately 58.2 kDa (Fig. 5A, lanes 1 and 2). We tested whether anti-apoptotic gene *Bcl-xL* could directly block the loss of MMP from B2-transfected cells. Direct observation of GL-av cells cotransfected with EYFP-B2 and EGFP-Bcl-xL revealed that the loss of fluorescence intensity was less in the EYFP-B2-transfected cells (Fig. 5B:d) than in the EGFP-Bcl-xL- and EYFP-B2-transfected cells at 24 h pt. The red fluorescence was also more intense (Fig. 5B:f; arrows),

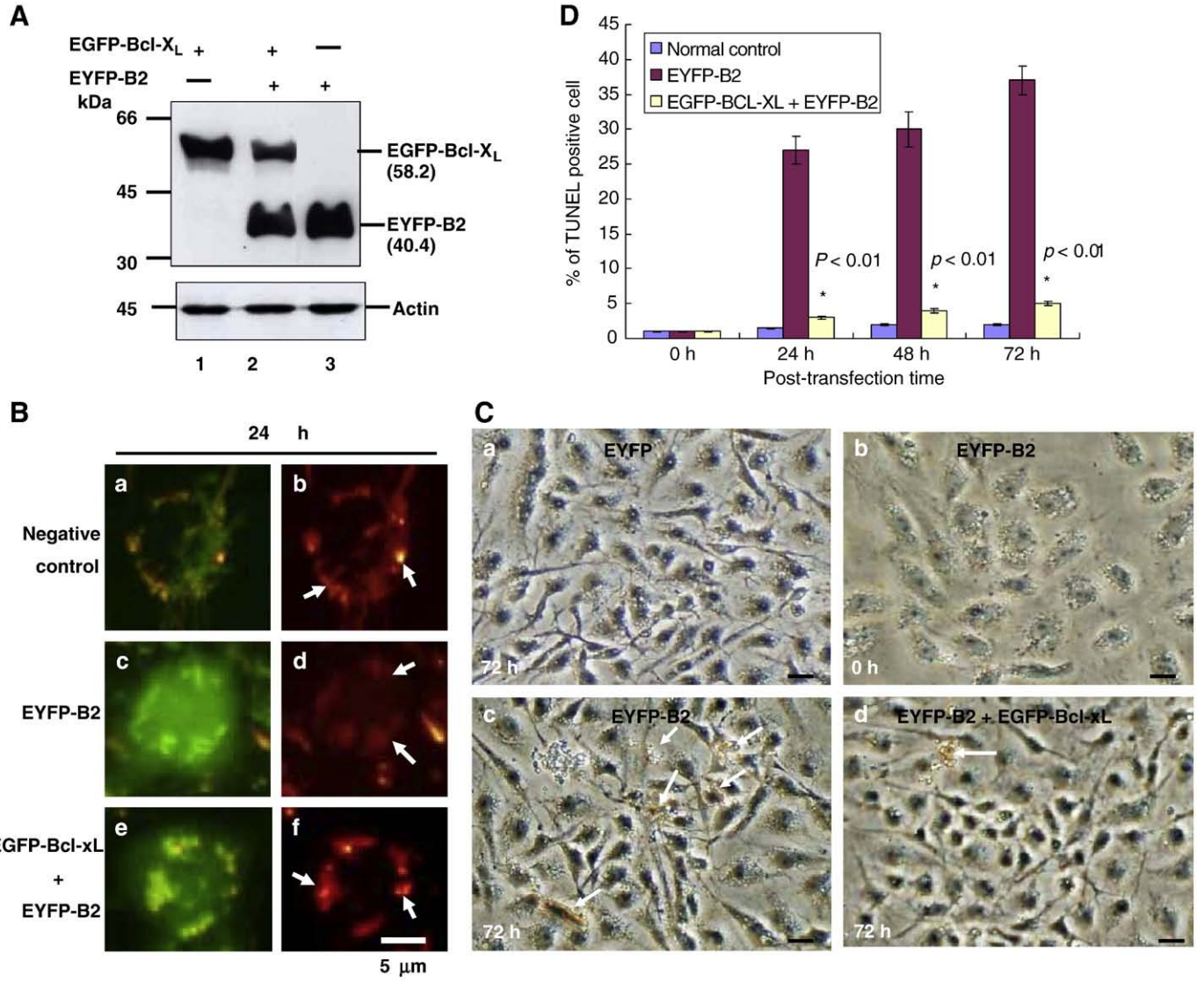

Fig. 5. zfBcl-x$_L$ blocked B2-induced mitochondrial disruption in fish cells. GL-av cells were transfected with pEYFP, pEYFP-B2, or co-transfected with pEYFP-B2 and Bcl-xL and incubated for 0, 24, 48 and 72 h. (A) Western blot analysis of Bcl-xL expression in lysates of GL-av cells transfected with RGNNV B2. GL-av cells transfected with Bcl-xL (lane 1), RGNNV B2 and Bcl-xL (lane 2), or RGNNV B2 (lane 3). Actin (internal control) is shown in Fig. 4A. (B) Mitochondria were labeled with the dye JC-1 and observed using fluorescence microscopy. The GL-av cells transfected with EYFP-B2 and EGFP-Bcl-xL were incubated for 24 h pt. Negative control cells (B:a and b); EYFP-B2-transfected GL-av cells (B:c and d); and EGFP-Bcl-xL- and EYFP-B2-transfected GL-av cells (B:e and f). Scale bar = 5 μm. (C) TUNEL staining demonstrated that Bcl-xL blocks RGNNV B2-induced apoptotic cell death in GL-av cells between 0 and 72 h as compared to cells lacking Bcl-xL. EGFP-transfected cells (C:a) at 72 h pt; EYFP-B2-transfected cells (C:b) at 0 h pt; EYFP-B2-transfected cells (C:c) at 72 h pt; and EGFP-Bcl-xL- and EYFP-B2- transfected cells (C:d and f) at 72 h pt. Bar = 10 μm. (D) Percentage of TUNEL-positive EGFP-, EYFP-B2-, and EYFP-B2- plus EGFP-Bcl-xL-transfected apoptotic GF-1 cells at different time points following transfection. Data were analyzed using either paired or unpaired Student's *t*-tests as appropriate. $p<0.01$ represented a statistically significant difference between the mean values of groups.

suggesting that Bcl-xL preserved MMP within the transfected cells. On the other hand, yellow–green fluorescence was observed within B2-transfected GL-av cells (Fig. 5B:c), indicating a loss of MMP, which severely reduced the red fluorescence (Fig. 5B:d; arrows). Negative control cells had light green and orange spots (Fig. 5B: a) and red fluorescence (Fig. 5B:b; arrows), indicating that these cells remained healthy.

TUNEL assays (Fig. 5C) were used to determine that Bcl-xL rescued B2-induced necrotic cell death (Fig. 5C:d; indicated by arrows) at 72 h pt as compared with the B2-transfected cells (Fig. 5C:c), vector control cells (Fig. 5C: a; at 72 h), and EYFP-B2-transfected cells at 0 h (Fig. 5C: b). The percent of TUNEL-positive nuclei (Fig. 5D) gradually increased in B2-transfected cells (1% at 0 h, 27% at 24 h, 30% at 48 h, and 37.5% at 72 h), but did not significantly increase in the Bcl-xL plus B2 cells (1% at 0 h, 3% at 24 h, 4% at 48 h, and 5% at 72 h) and negative control (vector-transfected) cells (1% at 0 h, 1.5% at 24 h, 2% at 48 h, and 2% at 72 h).

Knockdown of B2 blocked Bax upregulation and los of MMP in fish liver cells infected with RGNNV

We sought to define the genetic requirements for the potentially distinct death paradigm associated with loss-of-function due to B2 in GL-av cells after RGNNV infection. RNAi is a process of sequence-specific posttranscriptional gene silencing via double-stranded RNA (dsRNA) (McCaffrey et al., 2002; Elbashir et al., 2001; Kunath et al., 2003). Transfection with specific siRNA caused a 50% reduction in B2 expression at 12 h pi (Fig. 6A:a, lane 6), a 55% reduction at 24 h pi (Fig. 6A:a, lane 7), and a 35% reduction at 48 h pi (Fig. 6A:a, lane 8) as compared with the control group (siRNA

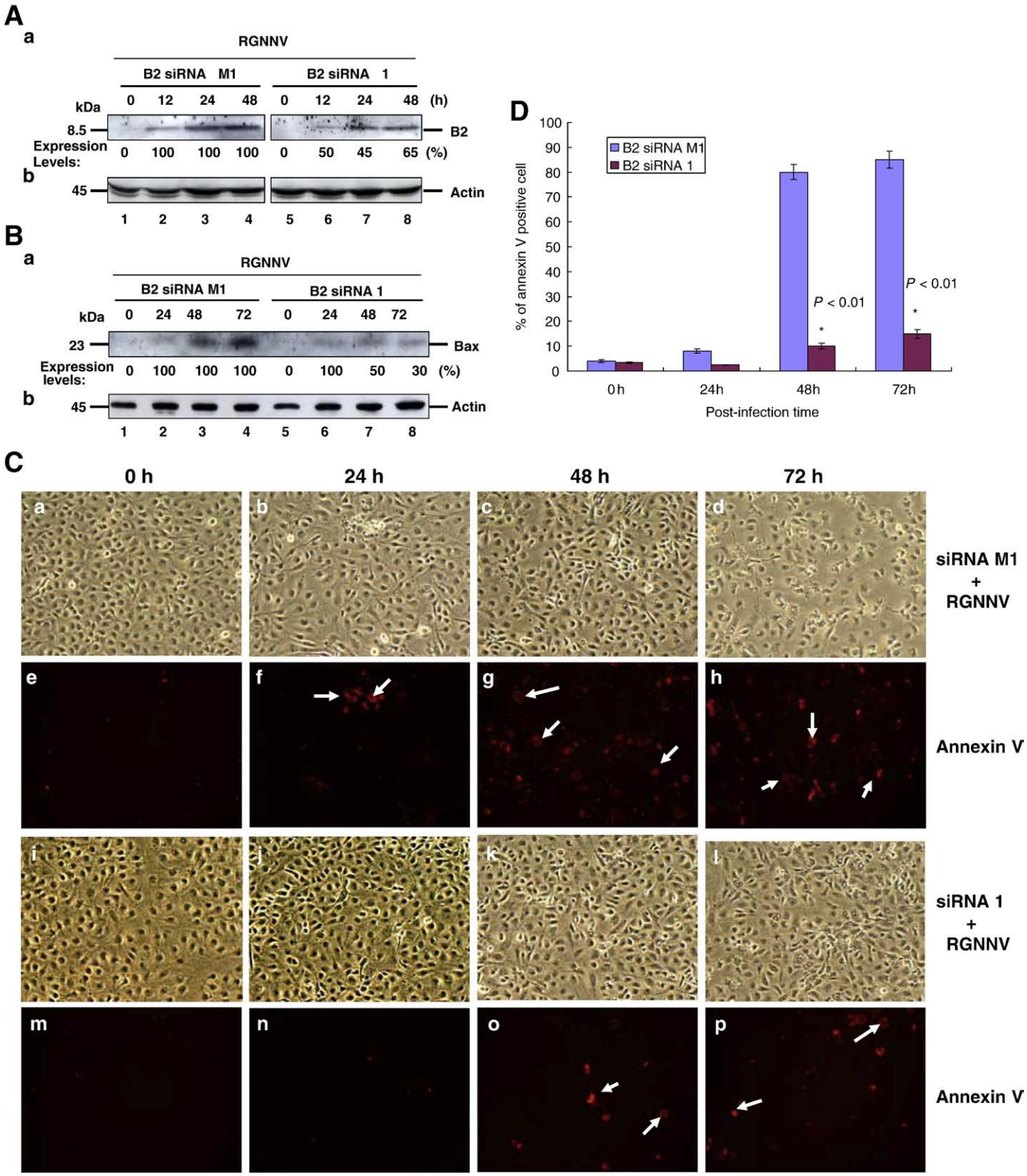

Fig. 6. Effective B2 knockdown following RGNNV infection was correlated with down regulation of Bax and prevention of PS exposure in fish cells. (A) B2-specific siRNA effectively knocked down *B2* expression, which was correlated with reduced expression of Bax (B), as determined by Western blot, which expression amounts were quantified by Personal densitometer (Molecular Dynamic) from A and B. (A:a) EYFP-B2 expression was reduced by B2 siRNA 1 at 0 h (lane 5), 24 h (lane 6), 48 h (lane 7), and 72 h (lane 8) pt, but not by B2 siRNA M1 at 0 (lane 1), 24 h (lane 2), 48 h (lane 3), and 72 h (lane 4) pt. The actin internal control is shown in A:b. (B:a) Bax expression was reduced by B2 siRNA 1 at 0 h (lane 5), 24 h (lane 6), 48 h (lane 7), and 72 h (lane 8) pt, but not by B2 siRNA M1 at 0 (lane 1), 24 h (lane 2), 48 h (lane 3), and 72 h (lane 4) pt. The actin internal control is shown in B:b. (C) Phase-contrast micrographs of Annexin V-stained, RGNNV-infected GL-av cells stably expressing either B2-specific siRNA M1 at 0 h (B: a and e), 24 h (B:b and f), 48 h (B:c and g), and 72 h (B: d and h) pt, or B2-specific siRNA 1 at 0 h (B:i and m), 24 h (B:j and n), 48 h (B:k and o), and 72 h (B:l and p) pt. Annexin V-positive cells (as necrotic cells) are indicated by arrows. (C) Data were analyzed using either paired or unpaired Student's *t*-tests as appropriate. p all <0.05 represented a statistically significant difference between the mean values of groups.

M1; Fig. 6A:a, lanes 2–4 at 12 h, 24 h, and 48 h pi, respectively) and the negative control group (Fig. 6A:a, lanes 1 (siRNA 1) and 5 (siRNA M1)). Actin expression was used as an internal control for the B2 siRNA M1 group (Fig. 6A:b, lanes 1–4) and for the B2 siRNA 1 group (Fig. 6A:b, lanes 5–8). The expression amounts were quantified by Personal densitometer (Molecular Dynamic) from Fig. 6A.

We next determined whether knockdown of B2 expression correlated with reduced expression of proapoptotic Bax in siRNA stable expression cells after RGNNV infection. Results showed that the induction of Bax expression was blocked by siRNA 1 following RGNNV infection. Bax expression was reduced 50% at 48 h pi (Fig. 6B:a, lane 7) and 30% at 72 h pi (Fig. 6B:a, lane 8). No reduction was observed in negative control siRNA M1 cells (Fig. 6B:a, lanes 1–4). Expression of the internal control actin is shown in Fig. 6B:b. The expression amounts were quantified by Personal densitometer (Molecular Dynamic) from Fig. 6B.

We also tested whether reducing B2 and Bax expression blocked RGNNV-induced cell death using the Annexin V assay. A more marked reduction in Annexin V-positive cells (Fig. 6C:m–p; arrows) was noted following RGNNV infection (moi=1) in cells with B2-specific siRNA 1 than in cells with B2-non-specific siRNA M1 (Fig. 6C: e–h; arrows). A greater increase in Annexin V-positive, RGNNV-infected (moi=1) cells (up to 60%) was noted following RGNNV infection in B2-specific siRNA M1-containing cells (4% at 0 h, 8% at 24 h, 80% at 48 h, 86% at 72 h pi) than in B2-specific siRNA 1-containing cells (3.5% at 0 h, 2% at 24 h, 11% at 48 h, 16% at 72 h pi) (Fig. 6C).

Finally, to determine whether siRNA could prevent the RGNNV-induced loss of MMP, siRNA was used to knock down B2 expression during RGNNV infection. Loss of MMP was more effectively blocked in infected GL-av cells stably expressing B2-specific siRNA 1 (25% loss reduced to 3% at 24 h pi, and 42.3% loss reduced to 3.5% at 48 h pi (Fig. 7B); Fig. 7A:d–f and j–l; indicated by arrows) than in RGNNV-infected cells expressing B2-specific siRNA M1 (Fig. 7A:a–c and g–i; indicated by arrows). On the other hand, we have checked the grouper *Mx* gene (the downstream gene of interferon I) expression level by RT-PCR in siRNA M1 cells. In the results, we did not detect it, which means stable-expression siRNA did not produce non-specific effects for up-regulation of *IFN-I* in the GF-1 cells (data not shown).

Discussion

Betanodaviruses infect a wide variety of larval and juvenile marine fish worldwide (Ball and Johnson, 1999), causing severe morbidity and mortality and significant economic losses to the aquaculture industry. Despite their severe economic impact, betanodaviruses are not well studied. In the present study, we demonstrate that the novel protein B2 can trigger mitochondria-mediated secondary necrotic cell death for viral spray. Characterization of betanodavirus molecular regulation processes may help in elucidating mechanisms of viral pathogenesis and infection.

Viruses have developed multiple strategies for manipulation of biological processes within infected cells through co-evolution with viral host species. Viruses can regulate cell proliferation, differentiation, and death (Yoshida, 2001; Seet et al., 2003). Meanwhile, many viruses inhibit apoptosis, a strategy that subverts one of the most ancient (non-immune) anti-viral mechanisms, namely the apoptotic suppression of infected cells. Suppression of apoptosis allows viruses to replicate before host cell die (Evertt and McFadden, 1999; Benedict et al., 2002). Moreover, viruses may induce apoptosis of either infected cells or immunologically relevant cells, with the purpose of increasing viral spread or subverting the host's immune response (Evertt and McFadden, 1999; Benedict et al., 2002).

In the present study, we sought to elucidate whether B2 expressed in the viral early replication stage functions as a Dicer antagonist for modulating the host siRNA defense system against viral gene expression, effectively enhancing viral replication. RNA interference constitutes a key component of the innate immune response to viral infection in plants, invertebrates, and mammals (Cullen, 2002; Fritz et al., 2006). It is now apparent that invertebrates, and more specifically nematodes and insects, also use RNAi to help control viral infection. Flock house virus (FHV), a member of the nodavirus family, can infect both insects and vertebrate cells. FHV infection of cultured drosophila cells results in the appearance of FHV-specific siRNAs and wild-type FHV infection is enhanced by disruption of the cellular RNAi response. RNAi is also important as an innate antiviral mechanism in intact insects (Wang et al., 2006; Galiana-Arnoux et al., 2006; Keene et al., 2004). In fish, on the other hand, the betanodavirus greasy grouper nervous necrosis virus B2 protein enhances the accumulation of betanodavirus RNA in infected mammalian cells (Johnson et al., 2004; Fenner et al., 2006). In our model system, B2 gene knock-down in grouper fish liver cells using synthetic B2 siRNA either markedly enhanced RGNNV viral RNA or increased viral protein expression (data not shown).

We have previously demonstrated that RGNNV induces apoptosis followed by secondary necrosis in GL-av cells and that loss of MMP in the mid-apoptotic stage may mediate this induction (Chen et al., 2006a). The necrotic process was blocked by the mitochondrial permeability transition pore inhibitor BKA, which may also act to rescue virus-infected cells (Chen et al., 2006a). Moreover, we have reported preliminary evidence showing that RGNNV-induced host cell death requires new protein synthesis (Chen et al., 2007). However, whether synthesis of viral proteins (B2 or protein α as a death inducer; Guo et al., 2003) or host proteins is essential remains unknown.

In the present study, we first examined whether a novel function of B2 could induce secondary necrosis in fish cells through a mitochondria-mediated death pathway. We found that over expression of B2 dramatically induced cell rounding and plasma membrane blebbing in EYFP-B2 expressing fish cells (Fig. 2B:f). Cells with these characteristics were also TUNEL positive, but were in a late apoptotic stage where secondary necrosis also occurred (Chen et al., 2007). How this novel necrotic *B2* gene regulates necrotic cell death during the middle and/or late replication stage is still unknown. We observed that B2 over expression induced the expression of the pro-apoptotic protein Bax at 48 h pt (Fig. 3, lane 7), which was correlated with loss of MMP during RGNNV infection, but not with upregulation of Bak (data not shown). Both proteins form heterodimers to create pore-like structures in the outer membrane of mitochondria that allow small solutes and water to enter the mitochondrial matrix during the induction of apoptosis (Garrido et al., 2006), perhaps resulting in mitochondrial disruption.

The Bcl-2 family of proteins includes both anti- and pro-apoptotic molecules and constitutes a critical, intracellular nexus for activating a common death pathway (Farrow and Brown, 1996). However, our observation that B2-induced cell death was directly blocked by zebrafish Bcl-xL indicates that Bcl-xL can block the loss of MMP following RGNNV infection in cells expressing Bcl-xL. Thus, interventions that mimic the effects of Bcl-xL and prevent the loss of MMP may be potent interventions in the treatment of viral infections in fish.

Our results suggest that the siRNA suppressor B2 may play a dual role during viral infections. This duality explains how a virus might effectively use one gene to modulate the host defense system (Iwamoto et al., 2005; Hamilton and Baulcombe, 1999) in early replication stages and also explains how B2 regulates host cell death for viral spread late in the replication cycle (Roulston et al., 1999). Our observations provide new insight into the function of B2 in cells from the animal (Iwamoto et al., 2005; Li et al., 2002; Lu et al., 2005), plant (Iwamoto et al., 2005; Li et al., 2002; Lu et al., 2005), and insect (Galiana-Arnoux et al., 2006) kingdoms.

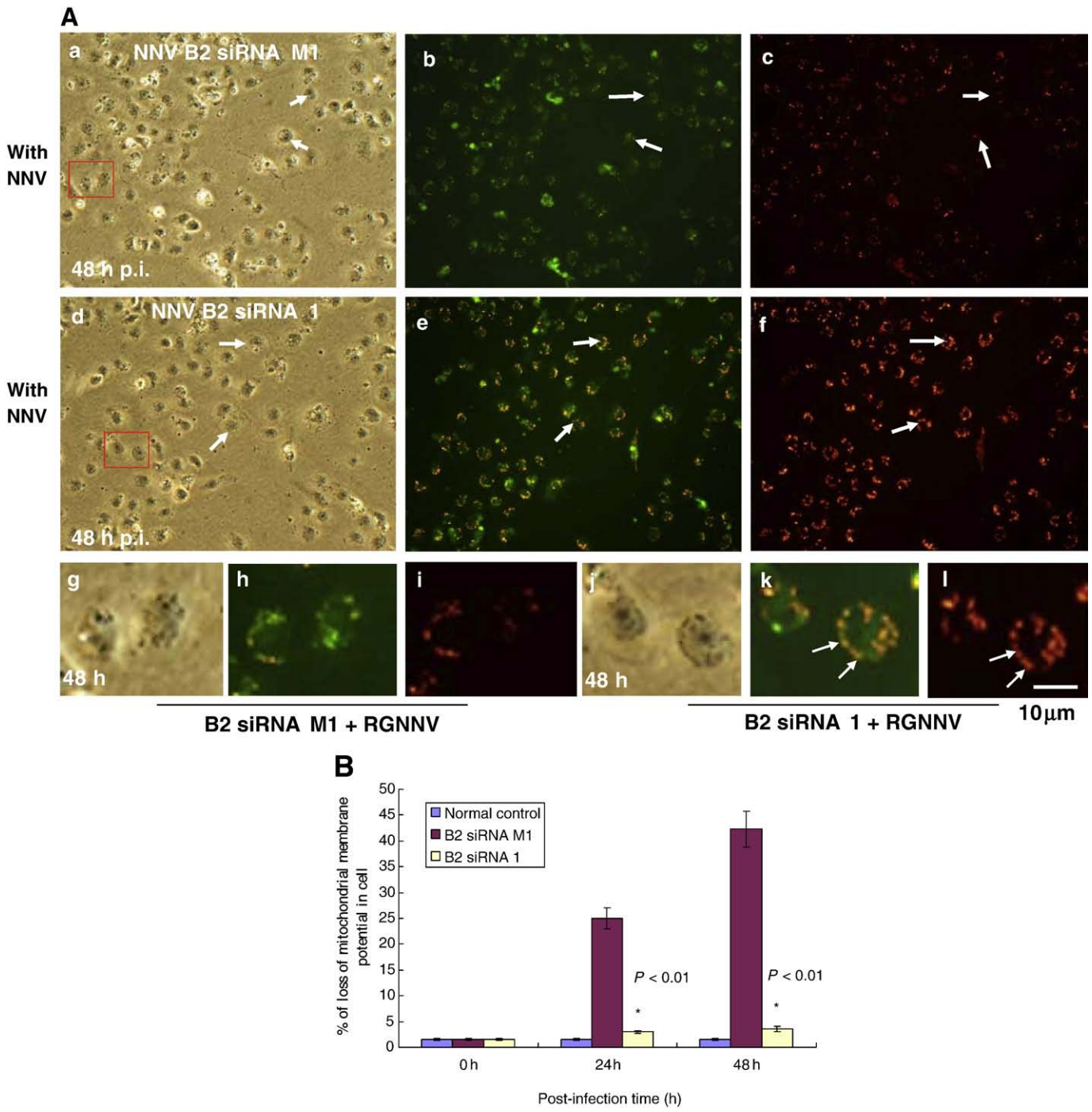

Fig. 7. Effective knockdown of B2 with RGNNV infection is correlated with prevention of the loss of MMP in fish cells. (A) RGNNV B2-specific siRNA 1 blocks B2-induced loss of MMP. Phase-contrast micrographs of MitoCapture dye-stained, RGNNV-infected GL-av cells stably expressing either the B2-specific siRNA M1 at 24 h (A:a –c; g-i are enlarged images of A:a–c) or the B2-specific siRNA 1 at 24 h (A: d–f; j–l are enlarged images of A:d–f) pt. Cells that have lost MMP are indicated by arrows (A:a–c). Increased orange (A:e and k) and red (A: f and l) fluorescence is indicated by arrows. Scale bar = 10 μm. (B) The percentage of MMP loss cell. The number of loss of MMP cells in 200 cells per sample was assessed in three individual experiments; each point represents the mean MMP loss of three independent experiments ± the standard error of the mean (SEM). Data were analyzed using either paired or unpaired Student's *t*-test as appropriate. A value of $p < 0.05$ was taken to represent a statistically significant difference between mean values of groups.

As summarized in Fig. 8, betanodavirus B2 could modulate the host siRNA response system at early stages in replication (0–12 h pi), and then at the middle stage (12–24 h pi) becomes a trigger for death signals through the upregulation of the proapoptotic Bax, which enhances MMP loss. Cells were disrupted in the late replication stage (24–48 h pi). In this Bax-mediated pathway, cell death was blocked by B2-specific siRNA, the anti-apoptotic protein Bcl-xL.

Materials and methods

Cell line and virus

The grouper liver cell line (GL-av) was subcloned from a grouper liver cell line (GL-a) obtained from Dr. Yang, Institute of Biotechnology, National Cheng Kung University, Taiwan, ROC. GL-av was

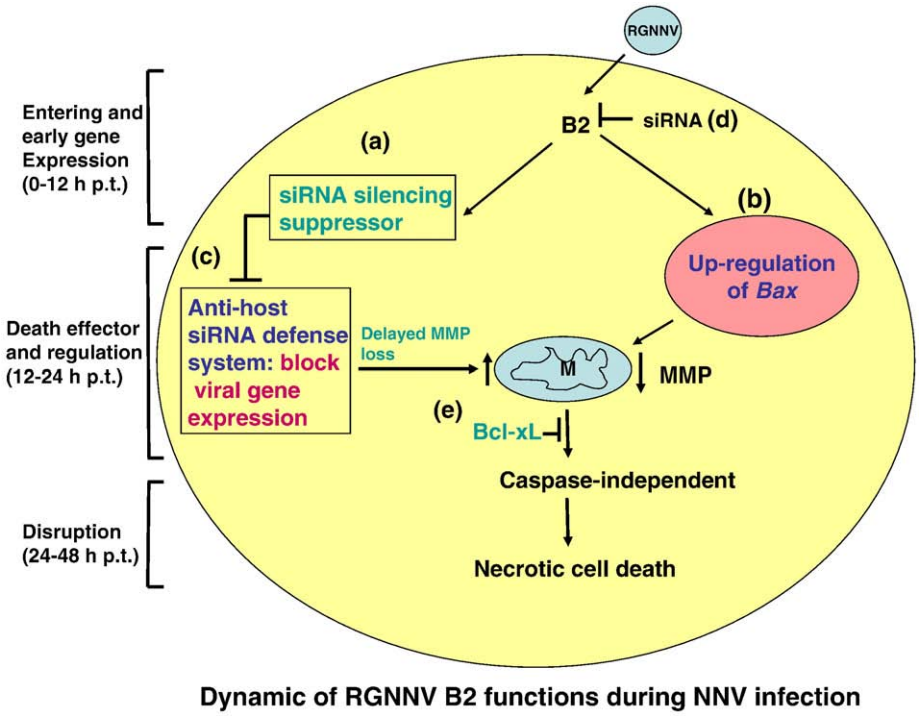

Fig. 8. A hypothesis of how the non-structural RGNNV protein B2 regulates the siRNA silencing system and secondary necrotic cell death. When a cell is infected with RGNNV, the virus binds to the cellular receptor, penetrates the cell, uncoats (the entry stage), and then expresses B2 to block the host siRNA silencing system (a) at early replication stage (0–12 h pt) in order to delay MMP loss and allow expression of other viral proteins (the gene expression stage; (c). During the regulation and effector stages (12–24 h pt; b), B2 can upregulate the pro-apoptotic gene *Bax* and affect mitochondria function and loss of MMP. In the disruption stage, phosphatidylserine (PS) and endonuclease are externalized and activate the cell's cytoskeleton: DNA is restructured and undergoes cleavage before the cell finally enters the post-apoptotic necrotic stage. The (a) B2 death function is halted by B2-specific siRNA (d) for knockdown of the B2 protein. Bcl-xL, an anti-apoptotic Bcl-2 protein (e), blocks loss of MMP and inhibits caspase-independent necrotic cell death.

grown at 28 °C in Leibovitz's L-15 medium (GibcoBRL, Gaithersburg, MD) supplemented with 5% fetal bovine serum and 25 μg/ml of gentamycin. Naturally infected red grouper larvae collected in 2002 in the Tainan prefecture were the source of RGNNV *T*ainan *No. 1* (RGNNV TN1) used to infect GL-av cells. The virus was purified as described by Mori et al. (1992) and was stored at −80 °C until use.

Cloning and sequence analysis of NNV B2

Synthesis and amplification of cDNA was carried out using the SuperScript One-Step™ reverse transcriptase-polymerase chain reaction (RT-PCR) system kit (Invitrogen, Carlsbad, CA) according to the manufacturer's instructions. NNV B2 primers P1 and P2 were each added to a final concentration of 0.2 μM. PCR cycling conditions were 54°C for 30 min, 2 min at 94 °C (to inactivate the reverse transcriptase), 95 °C for 30 s (DNA denaturation), 57 °C for 30 s (annealing), and 72 °C for 45 s (extension) for a total of 35–40 cycles. The RT-PCR primers NNV B2 P1 (5′-ACCATggAACAAA(G)TCCAACA-3′) and NNV B2 P2 (5′-CTAG(C)TCC(T)gTCTCCATCggC(T)T-3′) were used to amplify a fragment covering the variable region of *B2*. The purity and size of the amplified product was verified by 1.5% agarose gel electrophoresis and staining with ethidium bromide (Hong et al., 2002) The 228 bp, double-stranded cDNA was purified using the QIAquick™ gel extraction system (Qiagen, Valencia, CA) and subcloned using a pGEMT-easy cloning system (Promega, Madison, WI). The cloned PCR products were sequenced by the dye termination method using an ABI PRISM 477 DNA sequencer (Applied Biosystems, Foster City, CA) and scanned against the GenBank database BLAST (www4.ncbi.nlm.nih.gov/) and PROSITE (psort.ims.u-tokyo.ac.jp/) programs.

Expression of the B2 recombinant protein

Escherichia coli BL21(DE3)/pLysS cells were transformed with pET29a, which contained the B2 gene inserted at the EcoRI and Hind III sites. Cultures (50 to 200 ml) were incubated with 0.5 to 2.0 ml of preculture overnight. Optimal expression was obtained by induction with 1 mM IPTG (isopropyl-β-D-thiogalactopyranoside) when culture reached an optical density at 600 nm (OD_{600}) of 0.5. Expression of recombinant B2 was monitored by sodium dodecyl sulfate (SDS)-12% polyacrylamide gel electrophoresis (PAGE) (Laemmli, 1970), followed by staining with Coomassie brilliant blue R-250 (Lellouch and Geremia, 1999). For identification of the B2 protein using an N-terminus His tag, the gels were subjected to Western blot immunodetection (Kain et al., 1994). Blots were incubated with a 1:15000 dilution of anti-His tag polyclonal antibody followed by a 1:7500 dilution of a peroxidase-labeled goat anti-rabbit conjugate (Amersham Biosciences, Piscataway, NJ). Binding was detected by chemiluminescence and captured on Kodak XAR-5 films (Eastman Kodak, Rochester, NY). Cell pellets were resuspended in 4 ml of binding buffer (pH 7.8, 20 mM sodium phosphate, 500 mM NaCl) per 100 ml of cell culture. Lysozyme was added to a final concentration of 1 mg/ml and cell suspensions were incubated on ice for 30 min, and then incubated on a rocking platform for 10 min at 4 °C. A mixture of Triton X-100, DNase, and RNase was added to each suspension to a final concentration of 1%, 5 μg/ml, and 5 μg/ml, respectively, and incubated for an additional 10 min. The insoluble debris was removed by centrifugation at 3000 g (5000 rpm in a Sorvall SS-34 rotor) for 30 min at 4 °C. Supernatants were applied to $Ni2^{+}$ affinity columns (Qiagen) for binding on resin, and then columns were washed with 6 column volumes of binding buffer followed by 4 volumes of wash buffer (pH 6.0, 20 mM sodium phosphate, 500 mM NaCl). Bound

proteins were then eluted with 6 volumes of 10, 50, 100, and 150 mM imidazole elution buffer (pH 6.0, 20 mM sodium phosphate, 500 mM NaCl, 10 mM-150 mM imidazole) (Malabika et al., 2007). Eluted fractions were assayed for the presence of the polyhistidine-tagged protein by analyzing 20-μl aliquots by electrophoresis through a 10% SDS-polyacrylamide gel.

Preparation of a polyclonal antibody against B2

A New Zealand rabbit was subcutaneously immunized twice every 2 weeks with 500 μg/1.2 mL of purified recombinant B2 protein emulsified in an equal volume of Freund's complete adjuvant, boosted with 600 μg of antigen emulsified in an incomplete adjuvant at the seventh week. Thirty mL of blood was collected during the eighth week. Collected serum was precipitated with 50% $(NH_4)_2SO_4$, dialyzed against a 0.1 M phosphate buffer (PB), pH 8.0, and purified by protein A chromatography (Pharmacia). The immunoglobulin fraction eluted at pH 3.0 was collected and dialyzed against phosphate buffered saline (PBS). The eluted anti-B2 polyclonal antibodies were aliquoted and frozen at −70 °C. The column was reequilibrated with PB buffer containing 0.05% sodium azide (Hong et al., 1993).

Annexin-V-FLUOS staining

An analysis of phosphatidylserine on the outer leaflet of apoptotic cell membranes was performed using Annexin-V-fluorescein and propidium iodide (PI) to differentiate apoptotic from necrotic cells (Chen et al., 2007). After 0, 24, 48, and 72 h, a sample was removed from the culture medium and washed with PBS. The cells were incubated for 10–15 min with 100 μl of a HEPES-based Annexin V-fluorescein and PI staining solution (Boehringer-Mannheim, Mannheim, Germany). Evaluation was by fluorescence microscopy using a 488 nm excitation and a 515 nm long-pass filter for detection (Hong et al., 1998). The number of Annexin-V positive cells in 200 cells per sample was assessed in three individual experiments; each point represents the mean Annexin-V positive cells of three independent experiments±the standard error of the mean (SEM). Data were analyzed using either paired or unpaired Student's *t*-test as appropriate. A value of $P<0.05$ was taken to represent a statistically significant difference between mean values of groups.

TdT-dUTP labeling

For TdT-dUTP labeling, GL-av cells (10^6 cells/ml) were seeded on 35 mm diameter Petri dishes (New England Nuclear, MA) and incubated at 28 °C for 20 h. The negative control dishes received 2 ml of 5% fetal bovine serum in L-15 medium. The two treatment groups were incubated at 28 °C for 0, 24, 48, and 72 h, after which the cells recovered from the medium, washed with PBS, and fixed with freshly prepared paraformaldehyde solution (4% in PBS, pH 7.4) for 30 min at room temperature. Slides were washed with PBS and incubated with blocking solution (0.3% H_2O_2 in methanol) for 30 min at room temperature.

Petri dishes were rinsed with PBS, incubated after addition of permeabilization solution (0.1% Triton X-100 in 0.1% sodium citrate) for 5 min on ice, and rinsed twice with PBS. Next, 50 μl of TUNEL reaction mixture from an *in situ* cell death detection kit (Boehringer-Mannheim) was added to the sample and the Petri dishes were incubated in a humidified chamber for 60 min at 37 °C. Samples were either examined using a fluorescence microscope or by phase-contrast microscopy after signal conversion, which was accomplished by incubating samples with 50 μl of anti-fluorescein antibody conjugated with horseradish peroxidase (POD). Each Petri dish was incubated in a humidified chamber for 60 min at 37 °C and rinsed with PBS. Finally, 50–100 μl of diaminobenzidine (DAB) substrate solution was added for 10 min at room temperature. The Petri dish was then rinsed with PBS and a glass cover slip was placed in the bottom of the dish, which was examined by light microscopy (Hong et al., 1998). The number of TUNEL positive cells in 200 cells per sample was assessed in three individual experiments; each point represents the mean TUNEL positive cells of three independent experiments±the standard error of the mean (SEM). Data were analyzed using either paired or unpaired Student's *t*-test as appropriate. A value of $P<0.05$ was taken to represent a statistically significant difference between mean values of groups.

Identification of functions of EYFP-B2 fused genes in cell death

A B2 coding sequence from RGNNV B2 (B2 cDNA in pGEMT-easy plasmid) was amplified using the sense primer 5′-GAAGATCTAC-C**ATG**GAACAAATCCAA-3′ (Bag II site is underlined, the start codon of B2 is in boldface type) and an anti-sense primer 5′-CCCAAGCTTC-TAGTCCGTCTCCATCGG-3′ (Hind III site is underlined). After restriction digestion with *Bag*II and *Hind*III, the PCR product was ligated with an identically predigested pEYFP-C1 vector (ClonTech, Palo Alto, CA) to create pEYFP-B2. For cell transfection, 3×10^5 GL-av cells were seeded in 60 mm diameter culture dishes 1 day before the transfection procedure. The following day, 2 μg of either pEYFP or pEGFP-B2 was added using Lipofectamine-Plus (Life Technologies). Cell expression of the EYFP and EYFP fusion proteins for induction of cell death was visualized at the 24 h pt using FITC-filtered fluorescence microscopy.

Preparation of mitochondrial cytochrome c

For cell transfection, 3×10^5 GL-av cells were seeded in 60 mm diameter culture dishes 1 day before the transfection procedure. The following day, 2 μg of either pEYFP or pEGFP-B2 was added using Lipofectamine-Plus (Life Technologies). Samples were collected 24 and 48 h later and mitochondria were isolated as described previously (Shimizu et al., 2001). Briefly, 2×10^6 GL-av cells were washed with PBS and homogenized in 0.3 ml of mitochondria isolation buffer (0.35 M mannitol, 10 mM HEPES, 0.1% bovine serum albumin, pH 7.2) using a glass homogenizer. Unbroken cells and nuclei were pelleted by centrifugation (600 ×*g* for 5 min at 4 °C). The mitochondrial pellet was isolated from the centrifuged supernatant (10,000 ×*g* for 10 min at 4 °C) and the supernatant was collected and mixed with 25 μl of 10× SDS sample buffer. Samples (50 μl) were boiled and subjected to Western blot analyses.

Western blot analyses

GL-av cells were cultured by seeding 10^5 cells/ml in a 60 mm diameter Petri dish for 20 h prior to rinsing the monolayers twice with PBS, and then infecting with RGNNV (moi = 1) for 0, 24, 48, or 72 h pi at 28 °C. GL-av cells were transfected with pEYFP or pEYFP-B2 or cotransfected with pEYFP-B2 plasmids with Bcl-xL and incubated for 0 and 24 h. Alternatively, infected cells were stably transfected with pEYFP-B2 plasmid with B2-specific siRNA M1 (as a negative control) or B2-specific siRNA 1 and incubated for 0, 24 or 72 h. At the end of each incubation time, the culture medium was aspirated, the cells were washed with PBS, and the washed cells were lysed in 0.3 ml of lysis buffer (10 mM Tris, 20% glycerol, 10 mM SDS, and 2% β-mercaptoethanol, pH 6.8). An aliquot of the lysate was used for the separation of proteins by SDS-polyacrylamide gel electrophoresis (SDS-PAGE; Laemmli, 1970). The gels were subjected to Western blot immunodetection (Kain et al., 1994). Blots were incubated with a 1:1500 dilution of an anti-EGFP polyclonal antibody and then a 1:7500 dilution of a peroxidase-labeled goat anti-rabbit conjugate (Amersham Biosciences, Piscataway, NJ). Binding was detected by chemiluminescence and captured on Kodak XAR-5 films (Eastman Kodak,

Rochester, NY). The protein expression level amounts were quantified by Personal Densitometer (Molecular Dynamic).

Evaluation of mitochondrial membrane potential with a lipophilic cationic dye

GL-av cells (nontransfected or transfected with either pCDNA3.1 vector or pCDNA3.1-B2 plasmid in 60 mm diameter Petri dishes) were incubated at 28 °C for 0, 24, and 48 h pt. B2-specific siRNA M1 (as a negative control) and B2-specific siRNA 1 stable cell lines in 60 mm diameter Petri dishes were infected with RGNNV (moi=1) for 0, 24, and 48 h pi. The medium was discarded, 500 μl of diluted MitoCapture reagent (Mitochondria BioAssay™ Kit; BioVision, Mountain View, CA) was added, and each dish was incubated at 37 °C for 15–20 min (Chen et al., 2006a). The cells were examined immediately under a fluorescence microscope using the following band-pass filters: 488-nm excitation and 515-nm long-pass filter for detection of fluorescein; and 510-nm excitation and 590-nm long-pass filter for detection of rhodamine. The number of loss of MMP cells in 200 cells per sample was assessed in three individual experiments; each point represents the mean MMP loss of three independent experiments±the standard error of the mean (SEM). Data were analyzed using either paired or unpaired Student's *t*-test as appropriate. A value of $P<0.05$ was taken to represent a statistically significant difference between mean values of groups.

Selection of RGNNV B2-specific siRNA-containing cell lines

Using the psiLentGene vector (Promega, Madison, WI) as a template, the U6 promoter attached to a 19–22-nt sense strand of siRNA, a 9-nt loop (5′-TCTCTTGAA-3′), and a 19–22-nt antisense strand of siRNA were amplified by two-step PCR (Gou et al., 2003). The forward primer 5′ P_U6F (5′-CACCGAATTGGGTACCCGCTC-3′) used for all PCR steps was complementary to the 18 nt at the 5′-end of the U6 promoter. In the first round of PCR, the reverse 3′ primer 1–3 consisted of (5′) the 9-nt loop, a 19–22 nt antisense sequence, and the GGCC (3′) [(RGNNV TN1 B2 siRNA 1 (117–135) primer: 5′-GATGCGCACGTTCGTGATAAAGTTCTCTTATCACGAACGTGCGCATC-3′; and the RGNNV B2 siRNA M1 primer that contains eight points mutation from siRNA 1 as a negative control (indicated by underline): 5′-GACGAGTGCACTCAGGATAAAGTTCTCT TATCCTGAGTGCACTCGTC-3′)]. The reaction conditions were 95 °C for 3 min, 95 °C for 30 s, 60 °C for 40 s, 72 °C for 40 s, 35 cycles, and 72 °C for 10 min. RGNNV B2-specific siRNA 1 and siRNA M1 PCR products were digested with *Eco*RV and added to the psiLentGene vector. RGNNV B2-specific siRNA 1- and siRNA M1-producing cells were obtained by transfection of GL-av cells with the pRGNNV B2 siRNA 1 and pRGNNV B2 siRNA M1 vectors, respectively, and selection with G418 (800 μg/ml). In these vectors, transcription of insert sequences is driven by the immediate-early promoter of human cytomegalovirus. Selection time varied from 2.5–3 months (Chen et al., 2007), depending on cell-dependent properties.

Acknowledgments

The authors are grateful to Dr. Yang (Institute of Biotechnology, National Cheng Kung University, Taiwan, ROC) for providing the GL-a cell line. This work was supported by grants NSC 93-2313-B-006-003 and NSC 94-2313-B-006-002, awarded to Dr. Jainn-Ruey Hong from the National Science Council, Taiwan, Republic of China.

References

Ball, L.A., Johnson, K.L., 1999. Reverse genetics of nodaviruses. Adv. Virus Res. 53, 229–244.
Benedict, C.A., Norris, P.S., Ware, C.F., 2002. To kill or br killed: viral evasion of apoptosis. Nat. Immunol. 3, 1013–1018.
Bovo, G., Nishizawa, T., Maltese, C., Borghesan, F., Mutinelli, F., Montesi, F., DeMas, S., 1999. Viral encephalopathy and retinopathy of farmed marine fish species in Italy. Virus Res. 63, 143–146.
Chen, S.P., Yang, H.L., Her, G.M., Lin, H.Y., Jeng, M.F., Wu, J.L., Hong, J.R., 2006a. NNV induces phosphatidylserine exposure and loss of mitochondrial membrane potential in secondary necrotic cells, both of which are blocked by bongkrekic acid. Virology 347, 379–391.
Chen, S.P., Yang, H.L., Lin, H.Y., Chen, M.C., Wu, J.L., Hong, J.R., 2006b. Enhanced viability of a nervous necrosis virus infected stable cell line over-expressing a fusion product of the zfBcl-x_L and green fluorescent protein genes. J. Fish Dis. 29, 347–354.
Chen, S.P., Wu, J.L., Su, Y.C., Hong, J.R., 2007. Anti-Bcl-2 family members, zfBcl-x_L and zfMcl-1a, prevent cytochrome *c* release from cells undergoing betanodavirus-induced secondary necrotic cell death. Apoptosis 12, 1043–1060.
Cullen, B.R., 2002. RNA interference: antiviral defense and genetic tool. Nat. Immunol. 3, 597–599.
Delssert, C., Morin, N., Comps, M., 1997. A fish encephalitis virus that differs from other nodaviruses by its capsid protein processing. Arch. Virol. 142, 2359–2371.
Elbashir, S.M., Harhorth, J., Lendeckel, W., Yalcin, A., Weber, K., Tuschl, T., 2001. Duplexes of 21-nucleotide RNAs mediate RNA interference in cultured mammalian cells. Nature 411, 494–498.
Evertt, H., McFadden, G., 1999. Apoptosis: an innate immune response to virus infection. Trends Microbiol. 7, 160–165.
Falquet, L., Pagni, M., Bucher, P., Hulo, N., Sigrist, C.J., Hofmann, K., Bairoch, A., 2002. The PROSITE database, its status in 2002. Nucleic Acids Res. 30, 235–238.
Farrow, S.N., Brown, R., 1996. New members of the Bcl-2 family and their protein parters. Curr. Opin. Genet. Dev. 6, 45–49.
Fenner, B.F., Thiagarajan, R., Chua, H.J., Kwang, J., 2006. Betanodavirus B2 is an RNA interference antagonist that facilitate intracellular viral RNA accumulation. J. Virol. 80, 85–94.
Ferri, K.F., Kroemer, G., 2001. Organelle-specific initiation of cell death pathways. Nat. Cell Biol. 3, E255–E263.
Fritz, J.H., Girardin, S.E., Philpott, D.J., 2006. The structure of the flock house virus B2 protein, a viral suppressor of RNA interference, shows a novel mode of double-stranded RNA recognition. Science 339, pe27.
Galiana-Arnoux, D., Dostert, C., Schneemann, A., Hoffmann, J.A., Imler, J.L., 2006. Essential function in vivo for Dicer-2 in host defense against RNA viruses in drosophila. Nat. Immunol. 7 (6), 590–597.
Garrido, C., Galluzzi, L., Brunet, M., Puig, P.E., Didelot, C., Kroemer, G., 2006. Mechanisms of cytochrome c release from mitochondria. Cell Death Differ. 13, 1423–1433.
Gou, D., Jin, N., Liu, L., 2003. Gene silencing in mammalian cells by PCR-based short hairpin RNA. FEBS Lett. 548, 113–118.
Guo, Y.X., Wei, T., Dallmann, K., Kwang, J., 2003. Induction of caspase-dependent apoptosis by betanodaviruses GGNNV and demonstration of protein α as an apoptosis inducer. Virology 308, 74–82.
Hamilton, A.J., Baulcombe, D.C., 1999. A species of small antisense RNA in posttranscriptional gene silencing in plants. Science 286, 950–952.
Hong, J.C., Hong, T.H., Chang, J.G., Chang, T.H., 1993. Production and characterization of monoclonal antibodies against α and βspectrin subunits. J. Formos. Med. Assoc. 92, 61–67.
Hong, J.R., Lin, T.L., Hsu, Y.L., Wu, J.L., 1998. Aproptosis procedes necrosis of fish cell line by infectious pancreatic necrosis virus. Virology 250, 76–84.
Hong, J.R., Gong, H.Y., Wu, J.L., 2002. IPNV VP5, a novel anti-apoptotic gene of the Bcl-2 family, regulates Mcl-1 and viral protein expression. Virology 295, 217–229.
Iwamoto, T., Mise, K., Takeda, A., Okinaka, Y., Mori, K., Arimoto, M., Okuno, T., Nakai, T., 2005. Characterization of Striped jack nervous necrosis virus subgenomic RNA3 and biological activities of its encoded protein B2. J. Gen. Virol. 86, 2807–2816.
Johnson, K.N., Zeddam, L.L., Ball, L.A., 2000. Characterization and construction of functional cDNA clones of pariacoto virus, the first alphanodavirus isolated Australasia. J. Virol. 74, 5123–5132.
Johnson, K.L., Price, B.D., Eckerle, L.D., Ball, L.A., 2004. Nodamura virus nonstructural protein B2 can enhance viral RNA accumulation in both mammalian and insect cells. J. Viral. 78, 6698–6704.
Kain, S.R., Mai, K., Sinai, P., 1994. Human multiple tissue Western blots: a new immunological tool for the analysis of tissue-specific protein expression. BioTechniques 17, 982–987.
Keene, K.M., Foy, B.D., Sanchez-Vargas, I., Beaty, B.J., Blair, C.D., Olson, K.E., 2004. RNA interference acts as a natural antiviral response to O'nyong-nyong virus (Alphavirus; Togaviridae) infection of Anopheles gambiae. Proc. Natl. Acad. Sci. U. S. A. 101, 17240–17245.
Keep, O., Rajalingam, K., Kimmig, S., Rudel, T., 2007. Bak and Bax are non-redundant during infection- and DNA damage-induced apoptosis. EMBO J 26, 825–834.
Kunath, T., Gish, G., Lickert, H., Jones, N., Pawson, T., Rossant, J., 2003. Transgenic RNA interference in ES cell-derived embryos recapitulates a genetic null phenotype. Nat. Biotechnol. 21, 559–561.
Laemmli, U.K., 1970. Cleavage of structural proteins during the assembly of the head of bacteriophage T4. Nature 227, 680–685.
Lellouch, A.C., Geremia, R.A., 1999. Expression and study of recombinant ExoM, a β1–4 glucosyltransferase involved in succinoglycan biosynthesis in sinorhizobium meliloti. J. Bacteriol. 181, 1141–1148.
Li, H., Li, W.X., Ding, S.W., 2002. Induction and suppression of RNA silencing by an animal virus. Science 296, 1319–1321.
Lu, R., Maduro, M., Li, F., Li, H.W., Broitman-Maduro, G., Li, W.X., Ding, S.W., 2005. Animal virus replication and RNAi-mediated antiviral silencing in Caenorhabditis elegans. Nature 436, 1040–1043.
Lu, M.W., Chao, Y.M., Guo, T.C., Santi, N., Evensen, O., Kasani, S.K., Hong, J.R., Wu, J.L., 2008. Mol. Immunol. 45, 1146–1152.

Malabika, D., Ganguly, T., Chattoraj, P., Chanda, P.K., Bandhu, A., Lee, C.Y., Sau, S., 2007. Purification and characterization of repressor of temperate S. aureus phage phi11. J. Biochem. Mol. Biol. 40, 740–748.
McCaffrey, A.P., Meuse, L., Pham, T.T., Conklin, D.S., Hannon, G.J., MKay, A., 2002. RNA interference in adult mice. Nature 418, 38–39.
Mori, K., Nakai, T., Muroga, K., Arimoto, M., Mushiake, K., Furusawa, I., 1992. Properties of a new virus belong to nodaviridae found in larval striped jack (*Pseudocaranx dentex*) with nervous necrosis. Virology 187, 368–371.
Munday, B.L., Kwang, J., Moody, N., 2002. Betanodavirus infections of teleost fish: a review. J. Fish Dis. 25, 127–142.
Newton, K., Strasser, A., 1998. The Bcl-2 family and cell death regulation. Curr. Opin. Genet. Dev. 8, 68–75.
Oltvai, Z.N., Milliman, C.L., Korsmeyer, S.J., 1993. Bcl-2 hetrodimerizes in vivo with a conserved homolog, Bax, that accelerates programmed cell death. Cell 74, 609–619.
Poisa-Beios, L., Dios, S., Montes, A., Aranguren, R., Figueras, A., Novoa, B., 2008. Nodavirus increases the expression of Mx and inflammatory cytokines in fish brain. Mol. Immunol. 45, 218–225.
Roulston, A., Marcellus, R.C., Branton, P.E., 1999. Viruses and apoptosis. Annu. Rev. Microbiol. 53, 577–628.
Schneemann, A., Reddy, V., Johson, J.E., 1998. The structural and function of nodavirus particles: a paradigm for understanding chemical biology. Adv. Virus Res. 50, 381–446.
Seet, B.T., Hohnston, J.B., Brunetti, C.R., Barrett, J.W., Everett, H., Cameron, C., Sypula, J., Nazarian, S.H., Lucas, A., McFadden, G., 2003. Poxviruses and immune evasion. Annu. Rev. Immunol. 21, 377–423.
Shimizu, S., Matsuoka, Y., Shinohara, Y., Yoneda, Y., Tsujimoto, Y., 2001. Essential role of voltage-dependent anion channel in various forms of apoptosis in mammalian cells. J. Cell Biol. 152, 237–250.
Wang, X., 2001. The expanding role of mitochondria in apoptosis. Genes Dev. 15, 2922–2933.
Wang, X.H., Aliyari, R., Li, W.X., Li, H.W., Kim, K., Carthew, R., Atkinson, P., Ding, S.W., 2006. RNA interference directs innate immunity against viruses in adult Drosophila. Science 312, 452–454.
Wei, M.C., Zong, W.X., Cheng, E.H., Lindsten, T., Panoutsakopoulou, V., Ross, A.J., Roth, K.A., MacGregor, G.R., Thompson, C.B., Korsmeyer, S.J., 2001. Proapoptotic BAX and BAK: a requisite gateway to dysfunction and death. Science 292, 727–730.
Wu, H.C., Chiu, C.S., Wu, J.L., Gong, H.Y., Chen, M.C., Lu, M.W., Hong, J.R., 2008. Zebrafish anti-apoptotic protein zfBcl-xL can block betnodavirus protein α-induced mitochondria-mediated secondary necrosis cell death. Fish Shellfish Immunol. 24, 436–449.
Yoshida, M., 2001. Multiple viral strategies of HTLV-1 for dysregulation of cell growth control. Annu. Rev. Immunol. 19, 475–497.
Zamzami, N., Kroemer, G., 2001. The mitochondrion in apoptosis: how Pandora's box opens. Nat. Rev. Mol. Cell Biol. 2, 67–71.